Assessment of Electromagnetic Tracking Accuracy for Endoscopic Ultrasound

Ester Bonmati[1], Yipeng Hu[1], Kurinchi Gurusamy[2], Brian Davidson[2], Stephen P Pereira[3], Matthew J Clarkson[1,*], Dean C Barratt[1,*]

[1] UCL Centre for Medical Image Computing, Department of Medical Physics & Biomedical Engineering, University College London, London, UK
[2] Division of Surgery and Interventional Science, University College London, UK
[3] Institute for Liver and Digestive Health, University College London, UK

Abstract Endoscopic ultrasound (EUS) is a minimally-invasive imaging technique that can be technically difficult to perform due to the small field of view and uncertainty in the endoscope position. Electromagnetic (EM) tracking is emerging as an important technology in guiding endoscopic interventions and for training in endotherapy by providing information on endoscope location by fusion with pre-operative images. However, the accuracy of EM tracking could be compromised by the endoscopic ultrasound transducer. In this work, we quantify the precision and accuracy of EM tracking sensors inserted into the working channel of a flexible endoscope, with the ultrasound transducer turned on and off. The EUS device was found to have little (no significant) effect on static tracking accuracy although jitter increased significantly. A significant change in the measured distance between sensors arranged in a fixed geometry was found during a dynamic acquisition. In conclusion, EM tracking accuracy was not found to be significantly affected by the flexible endoscope.

Keywords: Electromagnetic tracking, endoscopic ultrasound, image-guided systems, accuracy, precision, validation

1 Introduction

Endoscopic ultrasound (EUS) imaging has become an increasingly important investigative tool in a number of endoscopic procedures, including bronchoscopy, endoscopic procedures involving the gastrointestinal tract, and for localising pancreatic lesions, for example during trans-gastric or trans-duodenal fine needle aspiration (FNA) or during the course of endoscopically guided treatments (endotherapy) [1]. However, many EUS-guided procedures are complex, technically challenging, and require significant experience [2]. The ability to track the 3D position and visualize the endoscope shape, and other surgical instruments inserted through it, in real-time is important for improving surgical confidence, reducing the skill required to navigate, and may ultimately allow a less experienced gastroenterologist to perform at an equivalent level as an expert. The additional navigational information becomes especially useful when combined with other diagnostic, planning, and intraoperative imaging modali-

* Joint senior author

ties, such as pre-operative X-ray computed tomography (CT) or magnetic resonance (MR) images, to provide anatomical context.

Electromagnetic (EM) tracking is arguably the most versatile option for computer-assisted interventions and therapy (CAI) as it allows flexible instruments inside the human body to be tracked in real-time using a very small sensor, and, unlike optical tracking or other image-based tracking methods, it does not require a line-of-sight to be maintained [3]. As a result, EM tracking has rapidly become the tracking method of choice for endoscopic interventions [4], and in turn for EUS-guided procedures [5, 6], and is now incorporated into a number of commercial navigation systems.

Several different protocols have been proposed to evaluate the accuracy of EM tracking systems, mainly to assess static errors [7–11]. The most common approach was proposed by Hummel et al. [8] and has been used to assess new EM systems [12, 13], the accuracy of sensors mounted on US probes [14, 15], and also for optimization [16]. This assessment protocol employs a machined base plate to measure positional and rotational tracking data, offering simplicity, reproducibility, a high precision ground truth and accuracy. This protocol is now widely considered to be the standard method, but there is the limitation that measurement accuracy is a function of translation or rotation [17]. Optical tracking [16] and robots have also been used, however, these solutions are expensive and typically involve complicated calibration procedures [10].

Despite the growing popularity of EM tracking in interventional applications, significant tracking errors due to metallic objects (i.e., steel, aluminium and bronze) placed between the emitter and the sensor, and the use of some electronic devices, such as a C-arm unit, have been reported to cause disturbances to the magnetic field below 4.2 mm [8, 13, 17–20]. Such errors can be particularly prevalent in clinical environments and their sources difficult to control. Therefore, it is challenging to predict the accuracy of an EM tracking system based on measurements from a different environment [21].

The aim of this study was to assess the precision and accuracy of two new EM sensor tools, designed for flexible endoscope tracking, by adapting Hummel et al. standardized protocol specifically for EUS-guided procedures. The main motivation was to determine the accuracy of a widely used EM tracking system when the sensor tools are placed alongside or inside an endoscope working channel, with an EUS probe turned off and on and, to better understand the errors associated with EM instrument tracking in the overall surgical navigation error analysis of EUS-guided procedures.

2 Materials

In this study, we evaluated a NDI Aurora® V3 Tabletop Field Generator (TTFG; Northern Digital, Inc., Waterloo, Ontario, Canada) with a tracking frequency of 40 Hz. This device has shown good performance in terms of accuracy and stability [12], which is required for guiding EUS-related procedures. The TTFG has an ellipsoidal volume of 600x420x600 mm starting at approximately 120 mm from the physical plane of the board. The manufacturer-reported accuracy of six degrees of freedom

(DOFs) sensor tools is 0.80 mm and 0.70° for positional- and rotational data, respectively, in terms of root-mean-square errors (RMSE)[1]. A NDI 6DOF catheter (Type 2) sensor tool, and a NDI 5/6DOF Shape tool (Type 1), were used, both of which are tools designed to be inserted in the working channel of a flexible endoscope. Results reported in this paper are based on tracking data acquired using the NDI Track software included in the NDI ToolBox (version 4.007.007).

To assess the tracking performance of EUS-guided procedures, we used an Aloka ProSound SSD 5000 ultrasound console with an Olympus GF-UCT240 endoscopic ultrasound transducer, operating at a frequency of 11 MHz. The endoscope has a working channel with a diameter of 3.7 mm.

A methacrylate Hummel board [8] with dimensions 550x650x12 mm was fabricated and used as a ground truth for static measurements. The board contains a grid of 10x12 holes with a precision of 10 µm at a temperature of 20°, spaced 50 mm apart in each direction, and a circle in the centre with 32 holes spaced 11.25° apart, with a radius of 50 mm. To reliably assess the variation along the z-axis of the reference coordinate system, and to enable comparison with older studies, we designed a modular marine plywood platform, which was rigidly secured above the TTFG. This platform allows the board to be easily positioned at three vertical z-levels (120 mm, 220 mm and 320 mm) from the origin of the global coordinate system (see **Fig. 1** (a)). Two acetal adapters were designed to position tracking tools and endoscopes on the board (see **Fig. 1** (b-c)). The tracking tool adapters included two pins at a distance of 50 mm that fit into a pair of holes in the board to fix the sensor or endoscope. The endoscope adapter also included four nylon screws to fix the endoscope and avoid undesired rotations or movement. Special attention was paid in using only plastic materials to avoid interference with the field emitted by the TTFG. Based on the tolerances of the fabrication of the phantom, the accuracy of the ground truth setup was estimated to be within 100 µm.

3 Methods

3.1 Static measurements

Using our setup, 72 positions on the grid for each of the three z-levels were available within the ellipsoidal TTFG working volume. For each grid position, 10 seconds of continuous positional and rotational data were acquired. For the purpose of comparison, measurements were recorded under three different conditions: a) the sensor in isolation, without the endoscope present (as a reference); b) the sensor inserted inside the working channel of the endoscope, with the ultrasound console turned off; and c) the sensor inside the working channel with the ultrasound console and transducer turned on. In order to fix the catheter sensor tool inside the working channel of the flexible endoscope, the tool was first inserted and fixed into a pushing catheter (see **Fig. 1** (d-e)). Afterwards, the pushing catheter was inserted into the working channel of the endoscope. For the convenience of interpretation of acquired rotational data,

[1] http://www.ndigital.com/medical/products/aurora/

the quaternions reported by the tracking system were converted to Euler angles, with rotations about the z-axis being first multiplied when the composite rotation matrices were constructed.

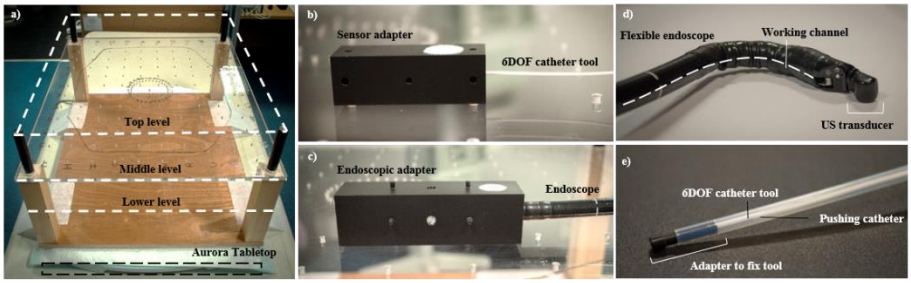

Fig. 1. Experimental setup. a) The modular platform with 3 positional levels placed above the Aurora Tabletop. b) Catheter tool sensor attached to the board with the tracking tool adapter. c) Flexible endoscope attached to the board with the endoscopic adapter. d) Flexible endoscope with a representation of the working channel. e) 6DOF catheter tool inserted in the pushing catheter and fixed with the adapter.

3.2 Precision

Repeated 3D tracking measurements for a static sensor tool contain random errors, commonly referred as *jitter*. For each sample, the Euclidean distance between the measured location and the mean location over all the samples was computed, whilst the rotational distance was calculated as the difference between each measured Euler angle and the mean angle. For each grid position, the precision was quantified by calculating the RMSEs of positional and rotational distances.

3.3 Accuracy

We adapted a distance-based measure to assess the accuracy of tracking based on the TTFG, similar to the one proposed in Hummel protocol [8]. For each grid position, we measured the distance to all of the other ones, which were available, at grid distances of 50 mm, 100 mm and 150 mm as suggested by the protocol (see Fig. 2 (a)). The accuracy was calculated as the mean of absolute difference between the ground-truth and the measured distance for each position. This measure provides an indication of how accurate the tracking is when the sensor is moved a certain distance away from a particular reference position. The accuracy along the z-axis, was defined as the mean of the absolute difference in distances between different vertical z-levels (i.e., bottom-middle, middle-top and bottom-top). Estimates of rotational accuracy were obtained by measuring all relative rotations of 11.25°, using the circle included in the board, at the three different levels. In this case, only one rotation was studied due to positioning restrictions of the endoscope adapter.

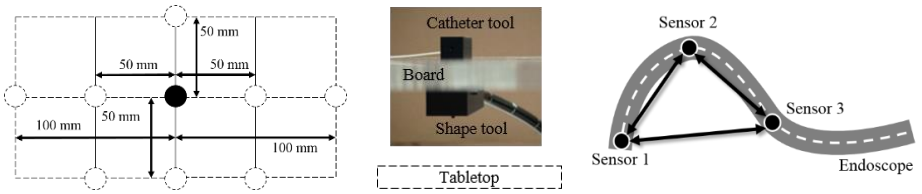

(a) (b) (c)

Fig. 2. a) Illustration of the accuracy measurements in terms of relative distances of 50 mm for rows and columns, and 100 mm for columns. b) Setup for the EUS-induced distortion error experiment. c) Position of the sensors inside the working channel to evaluate the dynamic error.

3.4 EUS-induced distortion error

During EUS-guided procedures, the endoscope can be used in conjunction with other sensors to track patient motion and/or other surgical tools. In particular, we were interested in assessing the effect of placing the endoscope between the TTFG and a sensor of interest (in this case, the catheter tool) which may affect the precision and accuracy of the tracking, as both the catheter and endoscope may cause distortion of the magnetic field. In this case, similar to Sections 3.2 and 3.3 but only for a small grid of 3x5 positions in the centre of the board, we first took static measurements without the endoscope (as a reference). We then repeated the experiment having attached the endoscope at the bottom of the board, just at the middle of the 3x5 grid positions, using the endoscopic adapter, such that the endoscope remained in a static position between the TTFG and the sensor of interest (see **Fig. 2** (b)). The grid positions were the closest to the endoscope, thus more likely to affect the tracking accuracy [8, 13, 18–20]. Additionally, the endoscope contained the shape tool in the working channel, and its position was measured as a reference of the distance between the two tracking tools. We then calculated the positional and rotational jitter, and the accuracy as defined in Sections 3.2 and 3.3.

3.5 Dynamic errors

To study dynamic error, the 6/5DOF NDI shape tool was inserted into the working channel of the flexible endoscope in a fixed position where the first three sensors (of 7) formed a triangle (see **Fig. 2** (c)). As a reference, 10 seconds of data were recorded in a static position and the mean position of each sensor was obtained. The endoscope was manually moved in a random path within the EM working volume while data was acquired continuously for 20 seconds. For each dynamic measurement, we calculated the distances between each pair of the three sensors which were located in the fixed part of the endoscope. These three distances were then compared with the corresponding mean distances computed from the reference measurements. This measure does not represent the complete "dynamic error" as any errors correlated between sensors, such as those caused by time latency, may cancel out each other. However, this is a simple and useful estimate of the relative dynamic error for applications where rela-

tive positions and distances are important, such as the real-time visualisation of the shape of a moving flexible endoscope.

3.6 Statistical Analysis

Paired two-sample Student's t-tests (t-tests), all with standard confidence level $\alpha=0.05$, were used to compare means of the static precision and accuracy errors between three scenarios (no endoscope, with endoscope and transducer off and with endoscope and transducer on). Additionally, because the errors were based on non-negative distance measures, results from nonparametric Kolmogorov-Smirnov tests (K-S tests) are also reported. In cases where any null hypothesis was rejected, i.e. a statistically significant difference was observed, a one-way analysis of variance (ANOVA) was used to further test if the three population means are likely to be the same. Furthermore, we used a Pearson's linear correlation coefficient (CC) to quantify the linear correlation between errors obtained from these different scenarios, and between the errors and the distance from the sampling location to the reference coordinate origin. Similarly, the t-test, K-S test and CC were used to analyse the EUS-induced distortion errors and the distance errors from dynamic acquisitions, described in Section 3.4 and 3.5, respectively, compared to their respective reference measurements.

4 Results

4.1 Precision

Each acquisition of 10 seconds led to a set of data with more than 400 valid samples. The mean and standard deviation of the positional and rotational jitter, obtained at the three different z-levels, are summarised in **Table 1** and **Table 2** respectively. Statistically significant difference was found between jitters with no endoscope and when the endoscope's transducer was turned off and on ($p\text{-value}<0.001$ and $p\text{-value}<0.001$, for t-test and K-S test, respectively). ANOVA also confirmed a statistically significant difference between three errors ($p\text{-value}=0.025$). Interestingly, positional jitters were correlated with a CC of 0.98 in both cases (both $p\text{-values}<0.001$). On the other hand, much smaller CCs were observed between rotational jitters (CC=0.34 and 0.35).

Table 1. Positional jitter averaged for all grid positions, at three different levels, with no endoscope and with the endoscope transducer turned on/off (mean ± STD in mm RMS).

Positional	Lower level	Middle level	Top level
No endoscope	0.01±0.01	0.04±0.01	0.14±0.03
Transducer off	0.01±0.01	0.04±0.01	0.15±0.04
Transducer on	0.02±0.01	0.05±0.01	0.18±0.04

Table 2. Rotational jitter averaged for all grid positions, at three different levels, with no endoscope and with the endoscope transducer turned on/off (mean ± STD in degrees RMS).

Rotational	Lower level	Middle level	Top level
No endoscope	0.02±0.03	0.06±0.03	0.17±0.07
Transducer off	0.12±0.26	0.07±0.03	0.18±0.07
Transducer on	0.33±0.38	0.10±0.05	0.72±0.70

Positional jitters versus Euclidean distance to the origin of the coordinates system is plotted in **Fig. 3**. A strong correlation was observed between jitters with all CCs greater than 0.89 for measurements from different grid positions and z-levels. Rotational jitters were correlated with the distance to the coordinate's origin with a correlation coefficient of 0.84 when there was no endoscope, a coefficient of 0.30 with the endoscope console turned off and 0.36 with the ultrasound transducer turned on. In this case, the lack of correlation between rotational precision and location was caused by the physical presence of the endoscope

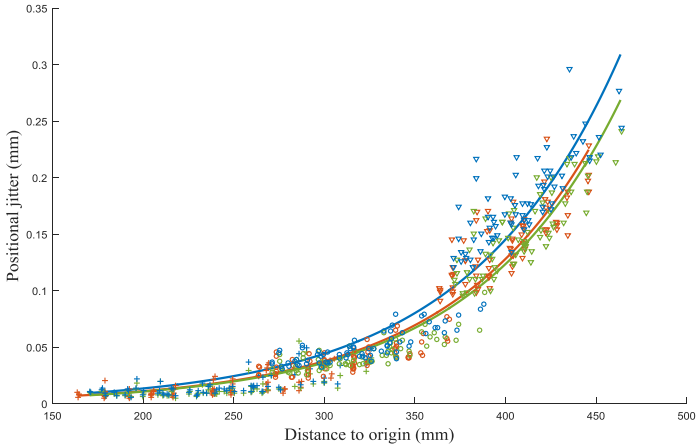

Fig. 3. Positional jitter versus Euclidean distance to origin of the coordinates system (+ = bottom level, o = middle level, ▼ = top level) with the corresponding exponential fitted curves without endoscope (orange), with the ultrasound transducer turned off (green), and with the ultrasound transducer turned on (blue).

4.2 Accuracy

For each z-level, a total of 52 values in rows and 56 values in columns were available at a distance of 50 mm, 32 values in rows and 40 values in columns were available at a distance of 150 mm, and finally, at a distance of 150 mm, 12 values in rows and 24 values in columns were obtained. Comparisons of the positional mean values are shown in **Fig. 4**. Overall, no statistically significant difference was found between the positional accuracy without endoscope and with endoscope and the ultrasound transducer on (ANOVA *p-value=0.496*). Positional accuracies with endoscope and no endoscope were correlated with a Pearson's coefficient higher than 0.81. Additional-

ly, there was no statistically significant difference between the distance from the low level to the top level and the sum of the distances between two adjacent levels (*p-value=0.740*, K-S test). Correlation analysis also showed a CC lower than 0.46 between the accuracy of each positon and the distance to the origin of the coordinates system in all cases.

The rotational accuracy results are summarized in **Table 3**. Overall, a statistically significant difference was found between the rotational accuracy without endoscope and rotational accuracy with endoscope (*p-value<0.001* and *p-value<0.001*, for t-test and K-S test, respectively). However, relatively low CCs were found between the accuracies without endoscope and with endoscope and the transducer on (CCs were 0.49 and 0.46 for the transducer on- and off cases, respectively).

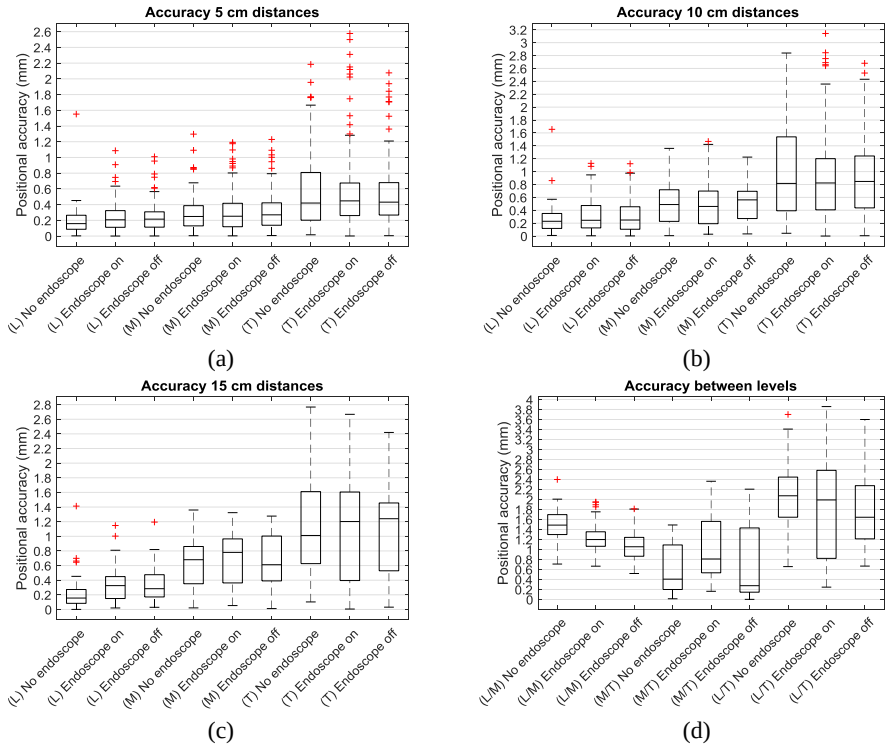

Fig. 4. Comparison of positional accuracy at a distance of 50 mm (a), 100 mm (b), 150 mm (c), and between levels (d). Boxplots show the absolute difference in distance (median, minimum, maximum, upper and lower quartile) for the bottom (L), middle (M) and top (T) levels.

Table 3. Relative rotational error averaged for all 32 positions, at three different levels, with no endoscope and with the endoscope transducer turned on/off (mean ± STD in degrees).

Rotational	Lower level	Middle level	Upper level
No endoscope	0.35±0.48	0.19±0.13	0.21±0.13
Transducer off	0.30±0.36	0.30±0.43	0.47±0.75
Transducer on	0.27±0.31	0.36±0.51	0.39±0.55

4.3 EUS-induced distortion error

The mean ± standard deviation of positional jitter for all grid positions was 0.03±0.01 mm without endoscope, and 0.02±0.00 mm when the endoscope was placed between the sensor and the TTFG (as described in Section 3.4). Rotational jitter was 0.05±0.01 mm without endoscope and 0.01±0.00 mm with endoscope. The distance between the shape tool, placed inside the endoscope, and the catheter tool ranged from 31.71 to 65.49 mm. Results showed no statistically significant difference in positional jitters with and without endoscope (*p-value=0.589*, K-S test) with a CC of 0.92. Rotational jitter was also not statistically significant different (*p-value=0.962* and *p-value=0.890*, for t-test and K-S test, respectively) with a CC of 0.76. A relatively poor correlation was found between the jitters and the distance to the endoscope (CC of 0.13 and -0.15, for positional and rotational jitter respectively).

Accuracy for 5 mm distances was 0.18±0.09 with no endoscope and 0.16±0.01 with endoscope. Statistical analysis showed no significant difference in accuracy with and without endoscope (*p-value=0.862*, K-S test).

4.4 Dynamic errors

The dynamic acquisition of 20 seconds led to 894 positional vectors acquired with an average speed of 0.31 m/s. Differences in distance, calculated between the three pairs of sensors (described in Section 3.5), were 0.29±0.42 mm, -0.39±0.24 mm and 0.64±0.4 mm. A histogram of the difference in distance between sensors is shown in **Fig. 5**. Dynamic distances where found to be significantly different than static distances (*p-value<0.001*, two-sample K-S test). The whole set of static measurements was also significantly different than the dynamic set of measurements (*p<0.001*, two-sample t-test). No strong correlation was observed between these three distance errors (CCs were -0.43, -0.18 and 0.09).

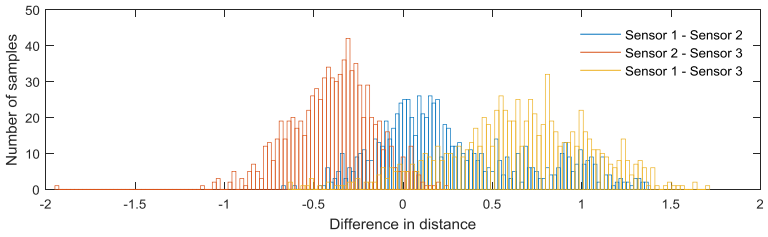

Fig. 5. Histogram of the differences in distance between the three fixed sensors during a dynamic acquisition.

5 Discussion

Positional accuracy did not significantly differ using the endoscope and there was no evidence of correlation with the distance to the TTFG. Our analysis shows clear evidence that the error obtained, when moving along the z-axis (away from the emitter), is cumulative. This effect was also observed with no endoscope. This error appears to

be systematic, thus, should be taken into account and corrected if possible. Rotational accuracy was also not strongly correlated with the distance to origin. Due to the limitation of the endoscopic adapter, only rotation about the Z axis was evaluated. This limitation may be overcome by creating two more adapters that allow rotation of the endoscope on the other two axes. On the other hand, positional jitter was found to significantly increase when the sensor was inserted in the working channel of the endoscope and was positively correlated with the distance to the origin of the coordinates system, remaining below 0.2 mm for all cases. Rotational jitter also increased, with a precision error of 0.7° in the worst case. In this case, no evidence was found regarding the correlation with the distance to the origin of the coordinates system.

EUS-induced distortion error was measured with the endoscope between the sensor and the TTFG. Our results showed no evidence of significant distortion when the endoscope was placed between 32 and 65 mm to the sensor. These positions were the closest on the grid to the endoscope during the experiments and therefore more likely to affect the accuracy. Thus, tracking other objects, such as clinical instruments, in combination with EUS seems feasible, although the accuracy of electromagnetic tracking should be quantified with the instrument of interest.

Errors introduced when the sensor is moving are of interest, although these have not been included in most assessment protocols reported in the literature [11]. In this work, we assessed a simple distance-based relative error between sensors during a dynamic acquisition, which was found to change significantly, with all mean errors below 0.7 mm. The dynamic error may affect the position and shape displayed of the flexible endoscopes during guidance, and its clinical impact will be dependent on the application.

The robustness of tracking accuracy with respect to the use of an endoscope was assessed by repeating the measurements with the EUS probe turned off and on, and without the endoscope being present. It is worth mentioning that the experiments were performed in a laboratory where conditions may differ from a clinical interventional suite, as the presence of other devices, such as a C-arm, may interfere in the measurements. To the best of our knowledge, no endoscope for EUS-guided procedures with an integrated EM sensor currently exists, although similar devices are available for bronchoscopy [22] and colonoscopy [23]. In addition, having the sensor tool inserted in the working channel has the advantages of portability and compatibility across different endoscope models and manufacturers compared with permanently embedding sensors within the wall of the flexible and/or bending sections. Our results suggest that it is possible to combine EUS and EM tracking without compromising the tracking accuracy significantly, although further research is required to estimate localisation errors for instruments, such as needle-tips, for specific clinical applications, which are likely to have different accuracy requirements.

This work focused on the study of static errors (jitter and relative accuracy), and partial distance-based dynamic errors, as we believe they are the main errors affecting the application of interest in EUS-guided procedures.

6 Conclusions

In this paper, we present the first accuracy study of 6DOF EM tracking tools inserted into the working channel of an endoscopic ultrasound probe, by using and extending a standardized protocol. Accuracy was not found to be highly affected by the endoscope for EUS-guided procedures, although the jitter increased. Future work includes evaluation of the tools in an interventional suite using different endoscopes as well as an assessment of the shape provided by the shape tool inserted in an endoscope.

Acknowledgment

This publication presents independent research supported by Cancer Research UK (CRUK) (Multidisciplinary Award C28070/A19985).

The authors would like to thank Joe Evans from the UCL department of Medical Physics and Biomedical Engineering for making and helping to design the accuracy assessment board, the supporting structures, and adapters.

References

1. Williams, D.B., Sahai, A. V, Aabakken, L., Penman, I.D., van Velse, A., Webb, J., Wilson, M., Hoffman, B.J., Hawes, R.H.: Endoscopic ultrasound guided fine needle aspiration biopsy: a large single centre experience. Gut. 44, 720–6 (1999).
2. Mertz, H., Gautam, S.: The learning curve for EUS-guided FNA of pancreatic cancer. Gastrointest. Endosc. 59, 33–37 (2004).
3. Mori, K., Deguchi, D., Sugiyama, J., Suenaga, Y., Toriwaki, J., Maurer, C.R., Takabatake, H., Natori, H.: Tracking of a bronchoscope using epipolar geometry analysis and intensity-based image registration of real and virtual endoscopic images. Med. Image Anal. 6, 321–336 (2002).
4. Fried, M.P., Kleefield, J., Gopal, H., Reardon, E., Ho, B.T., Kuhn, F.A.: Image-guided endoscopic surgery: Results of accuracy and performance in a multicenter clinical study using an electromagnetic tracking system. Laryngoscope. 107, 594–601 (1997).
5. Sumiyama, K., Suzuki, N., Kakutani, H., Hino, S., Tajiri, H., Suzuki, H., Aoki, T.: A novel 3-dimensional EUS technique for real-time visualization of the volume data reconstruction process. Gastrointest. Endosc. 55, 723–728 (2002).
6. Fritscher-Ravens, A., Knoefel, W.T., Krause, C., Swain, C.P., Brandt, L., Patel, K.: Three-dimensional linear endoscopic ultrasound—feasibility of a novel technique applied for the detection of vessel involvement of pancreatic masses. Am. J. Gastroenterol. 100, 1296–1302 (2005).
7. Frantz, D.D., Wiles, A.D., Leis, S.E., Kirsch, S.R.: Accuracy assessment protocols for electromagnetic tracking systems. Phys. Med. Biol. 48, 2241–2251 (2003).
8. Hummel, J.B., Bax, M.R., Figl, M.L., Kang, Y., Maurer, C., Birkfellner, W.W., Bergmann, H., Shahidi, R.: Design and application of an assessment protocol for

electromagnetic tracking systems. Med. Phys. 32, 2371–2379 (2005).
9. Wilson, E., Yaniv, Z., Zhang, H., Nafis, C., Shen, E., Shechter, G., Wiles, A.D., Peters, T., Lindisch, D., Cleary, K.: A hardware and software protocol for the evaluation of electromagnetic tracker accuracy in the clinical environment: a multi-center study. Proc. SPIE. 6509, 65092T–65092T–11 (2007).
10. Nagy, M.: Towards Unified Electromagnetic Tracking System Assessment — Static Errors. IEEE Eng. Med. Biol. Mag. 236, 1905–1908 (2011).
11. Franz, A.M., Haidegger, T., Birkfellner, W., Cleary, K., Peters, T.M., Maier-Hein, L.: Electromagnetic tracking in medicine -A review of technology, validation, and applications. IEEE Trans. Med. Imaging. 33, 1702–1725 (2014).
12. Maier-Hein, L., Franz, A.M., Birkfellner, W., Hummel, J., Gergel, I., Wegner, I., Meinzer, H.P.: Standardized assessment of new electromagnetic field generators in an interventional radiology setting. Med Phys. 39, 3424–3434 (2012).
13. Franz, A.M., Schmitt, D., Seitel, A., Chatrasingh, M., Echner, G., Oelfke, U., Nill, S., Birkfellner, W., Maier-Hein, L.: Standardized accuracy assessment of the calypso wireless transponder tracking system. Phys. Med. Biol. 59, 6797–6810 (2014).
14. Franz, A.M., März, K., Hummel, J., Birkfellner, W., Bendl, R., Delorme, S., Schlemmer, H.P., Meinzer, H.P., Maier-Hein, L.: Electromagnetic tracking for US-guided interventions: Standardized assessment of a new compact field generator. Int. J. Comput. Assist. Radiol. Surg. 7, 813–818 (2012).
15. Hastenteufel, M., Vetter, M., Meinzer, H.P., Wolf, I.: Effect of 3D ultrasound probes on the accuracy of electromagnetic tracking systems. Ultrasound Med. Biol. 32, 1359–1368 (2006).
16. Qi, Y., Sadjadi, H., Yeo, C.T., Hashtrudi-zaad, K., Member, S., Fichtinger, G.: Electromagnetic Tracking Performance Analysis and Optimization. 6534–6538 (2014).
17. Lugez, E., Sadjadi, H., Pichora, D.R., Ellis, R.E., Akl, S.G., Fichtinger, G.: Electromagnetic tracking in surgical and interventional environments: usability study. Int. J. Comput. Assist. Radiol. Surg. 10, 253–62 (2015).
18. Hummel, J., Figl, M., Kollmann, C., Bergmann, H., Birkfellner, W.: Evaluation of a miniature electromagnetic position tracker. Med. Phys. 29, 2205–2212 (2002).
19. Nixon, M.A., McCallum, B.C., Fright, W.R., Price, N.B.: The Effects of Metals and Interfering Fields on Electromagnetic Trackers. Presence Teleoperators Virtual Environ. 7, 204–218 (1998).
20. Kirsch, S.R., Schilling, C., Brunner, G.: Assesment of metallic distortions of an electromagnetic tracking system. In: SPIE Medical Imaging. International Society for Optics and Photonics (2006).
21. Yaniv, Z., Wilson, E., Lindisch, D., Cleary, K.: Electromagnetic tracking in the clinical environment. Med. Phys. 36, 876–92 (2009).
22. Leong, S., Ju, H., Marshall, H., Bowman, R., Yang, I., Ree, A.-M., Saxon, C., Fong, K.M.: Electromagnetic navigation bronchoscopy: A descriptive analysis. J. Thorac. Dis. 4, 173–85 (2012).
23. Szura, M., Bucki, K., Matyja, A., Kulig, J.: Evaluation of magnetic scope navigation in screening endoscopic examination of colorectal cancer. Surg. Endosc. 26, 632–8 (2012).